Characterising and Modelling Extended Conducted Electromagnetic Interference in Densely Packed DC-DC Converter

I Grobler[1] and MN Gitau[2]
Department of Electrical, Electronic and Computer Engineering, University of Pretoria, South Africa.
igrobler@csir.co.za[1], mgitau@postino.up.ac.za[2]

***Abstract*— High density high switching frequency power converter conducted EMC had been analysed, modelling the noise source and noise path, while providing accurate conducted EMC noise limits comparable to accredited noise measurements up to 100 MHz. The military specified DC-DC converters are applicable, spanning from 100 W handheld power managers up to 2 kW DC-DC battery chargers. Circuit layout high frequency effects as well as high frequency impedances of the power components were characterised. The effect of a higher switching frequency was demonstrated. At first, a trapezoidal noise source and lumped element noise path model was adopted, showing high frequency limitations of this technique. Thereafter, a lumped element model including a switching component was created. A Transient model circuit analysis was investigated to represent circuit noise as measured with a LISN. Common mode and differential mode signals were extracted in both the simulated results and the bench measurements.**

Keywords—EMC; High Switching Frequency; Lumped Element EMC Model.

I. INTRODUCTION

It is preferable to make the EMI management of a power converter an integral part of the design process and thus optimise the converter system design. This will improve the overall design efficiency and shorten the crucial time to market period [1]. It is of utmost importance to try and model the electromagnetic compatibility concurrent with the power processor design stage. The marketplace is in need of an affordable accurate and practical EMI modelling and prediction method suitable to be used as a design tool [2]. Furthermore, the modelling output should be comparable to the actual accredited measurements building confidence in qualifying the converter design.

The new generation high density power processors, passive as well as active devices, are in close proximity to each other. This close proximity results in the enhancement of parasitic capacitance and inductive coupling, creating a complex high frequency electromagnetic environment. Furthermore, switching frequencies have been dramatically increased leading not only to reduced passive component values, but also greater EMI levels shifting to higher frequencies, resulting in conducted EMC disturbance. Component parasitics and magnetic or electrostatic coupling effects can therefore not be neglected.

Performing extended conducted electromagnetic interference tests beyond the 30 MHz limit is of significant value. It is a far easier test than radiated testing and will show noise phenomena that could eventually become more complex radiated problems. With this knowledge, the belief is that if conducted EMI can be contained by firstly, understanding the mechanism thereof, and secondly, by designing for minimum conducted emissions over the extended band, the radiated emissions that are more difficult to analyse, could also be adequately lowered in the process.

Most affordable EMI models, due to simplification and as a result of the techniques used, deal only with the lower end of the frequency range. To deal with both low and high frequency conducted EMI noise, a more accurate modelling methodology is required [1,2,3]. The use of PowerSim, in conjunction with MatLab, was used as power converter design tool with subsequent conducted emission investigation. A similar technique is reported in [4] using Whole-Link circuit models which tested up to 30 MHz. Another attempt, reported in [5], used ORCAD circuit analysis, but omitted the high frequency models of the power components which resulted in poor simulation accuracies.

II. THEORY

A. Conducted Emission Modes

Two main conducted emission modes exist, the differential mode of conduction and the common mode of conduction as defined in Fig. 1. Differential mode (DM) noise is mainly caused by the current flow in the circuit. DM propagation path is normally made up of the dc-link capacitors, high frequency capacitors, the bus bars or tracks, and connectors such as screw terminals. Common mode (CM) noise is dictated by the voltage amplitude of the switching signal [6]. CM propagation path is made up mainly of the parasitic capacitance between the bus bars or tracks and the ground plane, and the parasitic capacitance between the switching device and the ground plane, of which the latter is normally separated by a thin insulator. Noteworthy is that the common mode loop comprises

of the larger loop area, prone for noise susceptibility and radiation at higher frequencies [7].

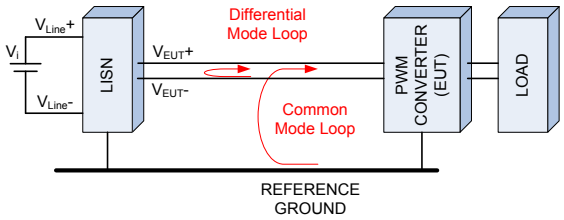

Fig. 1: Common Mode and Differential Mode Noise Defined

B. *High Frequency Analysis*

Modern switch mode converter units and motor drive systems use high speed semiconductor devices such as IGBT's and MOSFETs. The trend towards smaller packaging, higher densities, improved performance, reduced weight and lower cost require high switching frequencies and higher dv/dt and di/dt for lower switching losses. The higher switching frequencies cause higher levels of interference moving into a higher frequency band than previously anticipated.

The trapezoidal wave is seen as the noise source. The high frequency effect can be shown analyzing the waveform.

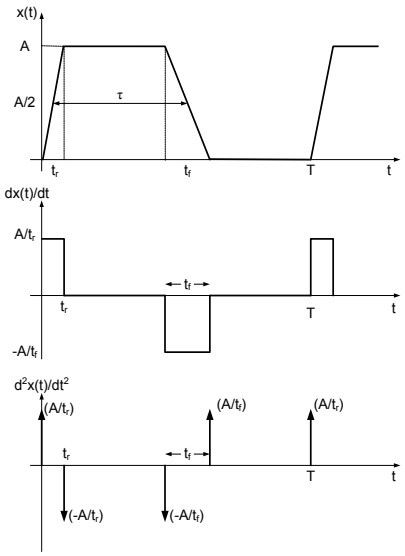

Fig. 2: Trapezoidal Wave and its Expansion Coefficients

The expansion result is given in (1).

$$\left|C_n^+\right| = 2 \cdot A \cdot \frac{\tau}{\mathrm{T}} \cdot \left|\frac{\sin(n\pi\tau / \mathrm{T})}{n\pi\tau / \mathrm{T}}\right| \cdot \left|\frac{\sin(n\pi\tau_r / \mathrm{T})}{n\pi\tau_r / \mathrm{T}}\right| \quad (1)$$

$$for \quad n \neq 1, \qquad t_r = t_f$$

Plotting the spectral bounds can show that an increase in high frequency noise occurs when the switching frequency increases (T2 > T1) as well as when the rise/fall times of the trapezoidal wave increases (tr2 > tr1).

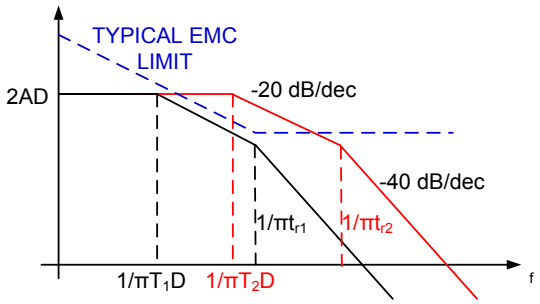

Fig. 3: Trapezoidal Wave Spectral Bounds

The higher the frequency, the easier the noise path transmits through the power converter. The switching inductor stray capacitance impedance decreases with frequency making way for easier high frequency passage. The effective series inductance impedance of the filter capacitors increases with frequency, shunting less noise to ground. Fig. 4 shows the ringing waveform imposed on the trapezoidal signal, and the consequent increase in the noise spectrum.

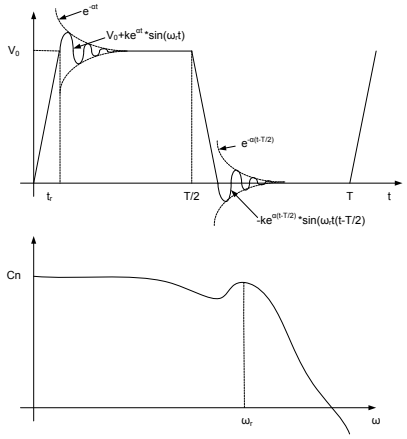

Fig. 4: Ringing Effect on Switching Signal

Fig. 5 shows a measurement of a Gallium Nitride MOSFET converter, increasing the switching frequency in steps from 50 kHz to 2 MHz. The switching frequency harmonic moves higher up in the spectrum, with reduced amplitude, but the high frequency effects increase in noise levels due to higher frequency components in the noise generation signal and easier transmission through the noise path.

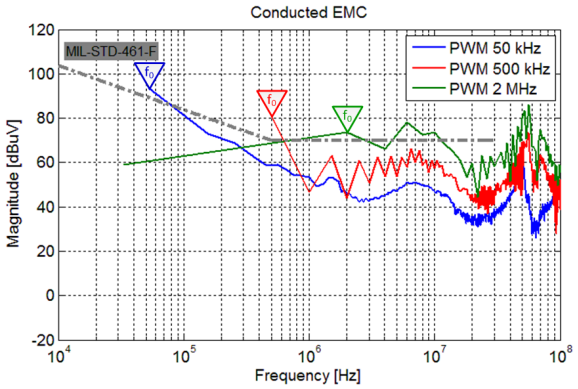

Fig. 5: Increased Switching Frequency Noise Spectrum

III. MODELLING FOR EMC

Modelling for conducted emissions, a step-down circuit will be analysed and verified. The schematic together with the LISN circuit is shown in Fig. 6.

A. Simplified Model

The simplified model for the circuit in Fig. 6 is shown in Fig. 7 and Fig. 8, consisting of a trapezoidal noise source and lumped element noise path, was investigated for accuracies. This type of conducted EMC analysis occurs frequently in literature [6].

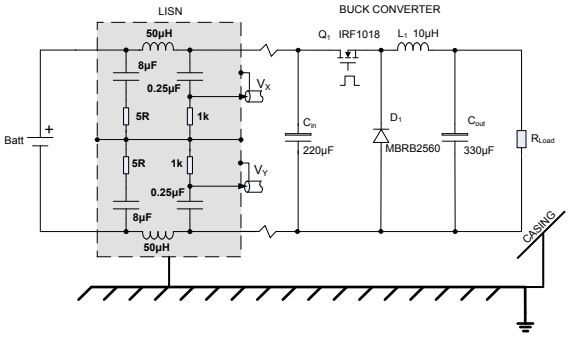

Fig. 6: Step-Down Circuit

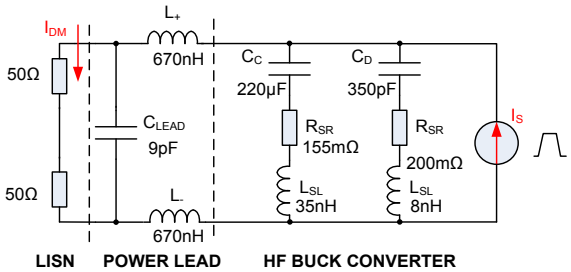

Fig. 7: Simplified DM Model

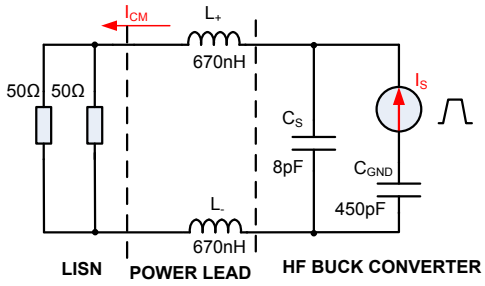

Fig. 8: Simplified CM Model

The analysis of the circuit in Fig. 7 and fig. 8 will be given. The one-sided Fourier transform of the Differential Mode (DM) LISN voltage can now be expressed as:

$$\left| V_{DM}(j\omega) = \sum_{n=1}^{\infty} 2 \cdot |C_n| \cdot \delta(\omega - \omega_n) \right| \tag{2}$$

The complex Fourier expression is represented by C_n and δ is the unit impulse function (Dirac-delta function) and $\omega_n = n.\omega_0$ where ω_0 is the angular switching frequency in rad/s. The coefficients C_n are computed as follows:

$$|C_n| = \frac{1}{T \cdot \sqrt{2}} |I_S(j\omega_n) \cdot H_{DM}(j\omega_n)| \tag{3}$$

The coefficients are those obtained for a trapezoidal waveform. For special cases where the rise time t_r and the fall time t_f are equal, the trapezoidal waveform can be simplified as follows:

$$I_S(j\omega) = A\frac{\tau}{T} \cdot \frac{Sin(n\omega_0\tau/2)}{n\omega_0\tau/2} \cdot \frac{Sin(n\omega_0\tau_r/2)}{n\omega_0\tau_r/2} \cdot e^{-jn\omega_0(\tau+t_r)/2} \tag{4}$$

$H_{DM}(j\omega_N)$ represents the transfer function from the equivalent current source $I_s(s)$ to the LISN voltage, or $V_{DM}(j\omega_N)$.

The one sided spectral envelope can now be expressed in dBµV as:

$$S_{DM}(j\omega_n) = 120 + 20 \cdot \log(2 \cdot |C_n|) \tag{5}$$

Similar Equations can be generated for the common mode spectral envelope.

The circuit in Fig. 6 has been prototyped and a noise measurement was performed with the LISN. This result can be compared with the simplified analysis.

The results are shown in Fig. 9 and Fig. 10. The low frequency band spectral plot shows very good comparison to practical measurements, but the high frequency results are not accurate. Improving the accuracy of the simplified model can be achieved by replacing the trapezoidal signal with the actual switching signal. This improves the high frequency accuracy, but it turns out to be a time consuming exercise whilst the detail of the switching signal is only available when the circuit is prototyped.

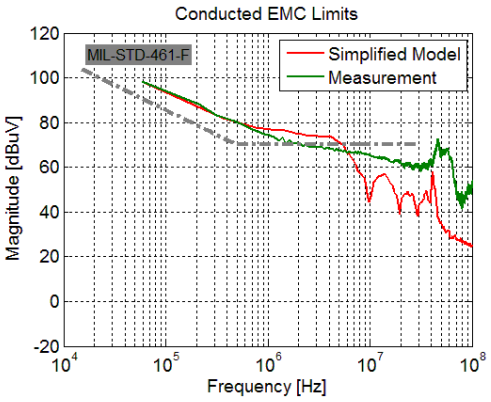

Fig. 9: DM Simplified Model Spectral Slope

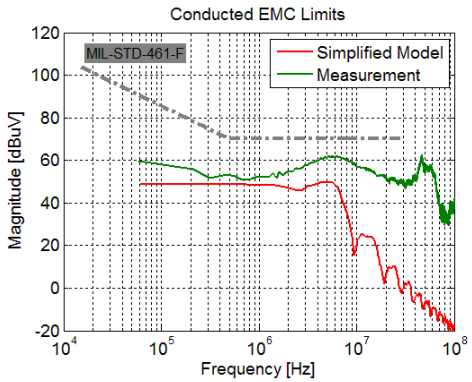

Fig. 10: CM Simplified Model Spectral Slope

B. *High Frequency Model*

The step-down circuit in Fig. 5 has been drawn out in PowerSim, replacing all components, including the switches, passive components and leads, with high frequency equivalent circuits. The feed cable from the LISN to the converter has been characterized with an impedance analyser.

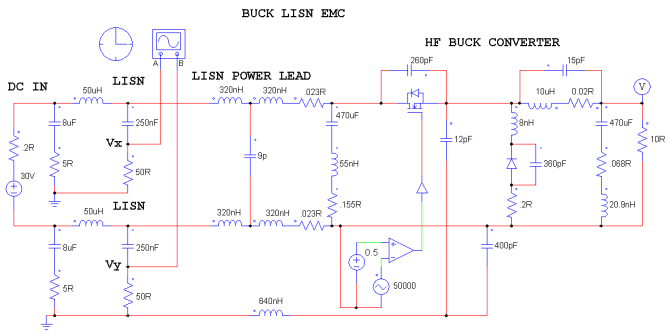

Fig. 11: PowerSim Circuit Model

The MOSFET and diode capacitance to the heatsink was measured to be 12 pF, but can be calculated very accurately with the following capacitor equation:

$$C_{Heat\sin k} = \frac{\varepsilon_0 A}{d} \qquad (5)$$

where ε_0 is the permittivity of the insulator, A the area of the MOSFET tab and d the insulator thickness.

The dc capacitors as well as the switching inductor were also characterised with an impedance analyser. The LISN is a standard MIL-STD-461-F circuit. The test method is from the same document, specifying a conductive ground plane for the converter.

The simulated time plot from the Vx port is shown in Fig. 12, showing the prominent frequencies occurring through the switching cycle in red and the switching signal in blue.

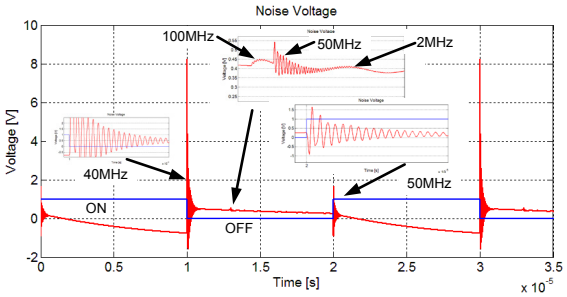

Fig. 12: Simulated Time Signal at LISN Port

The LISN port signals are then imported and converted in MATLAB performing the CM and DM calculations and subsequent spectral plot. Fig. 13 shows the FFT from the LISN ports as well as the extraction of the CM and DM signals.

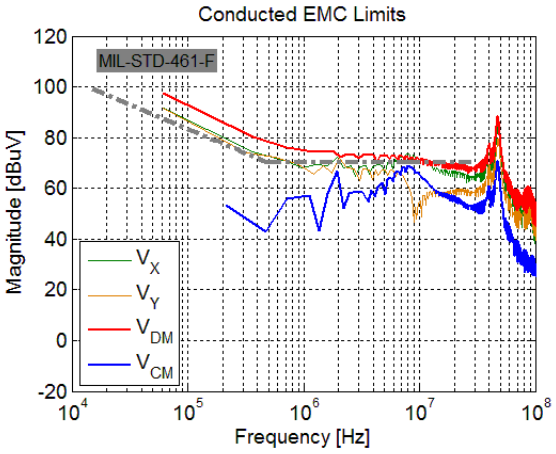

Fig. 13: Modelled Spectral Plot for Down Converter

The above plots are the basic high frequency lumped element version. In general and as reported in literature [4] [5], the traditional lumped element analysis suffers from convergence errors (mostly from Microcap users) and long analysis time. PowerSim on the other hand, reaches the steady state in a few seconds. The data file is exported to MATLAB and an FFT performed. This quick turnaround time for conducted emission results can be easily incorporated in the overall design of the power converter. On the contrary, the high

frequency model in PowerSim can be used for further stability analyses and component limit verification, not necessarily incorporated in the normal power design phase circuit.

Due to the quick simulation time, the circuit can be easily twigged against the actual measurements to incorporate coupling effects, broadening the insight into the noise mechanisms.

IV. MEASUREMENTS

The step-down circuit in Fig. 6 has been prototyped to verify the simulated results. The circuit prototype is shown in Fig. 14. The input voltage was set to 50 V. The output was tuned to 30 V dissipating power into a 10 Ω resistor.

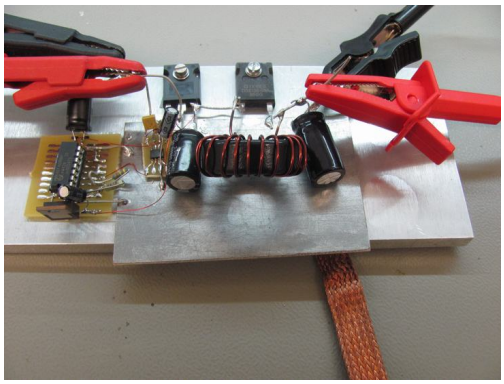

Fig. 14: Step-Down Test Circuit

The bench setup is shown in Fig. 15. Great care was taken to compare and validate the bench to an accredited EMC facility for accurate measurements. A LINDGERN coil was used to verify the CM and DM extraction calculations from the digital recording of the Vx and Vy LISN ports.

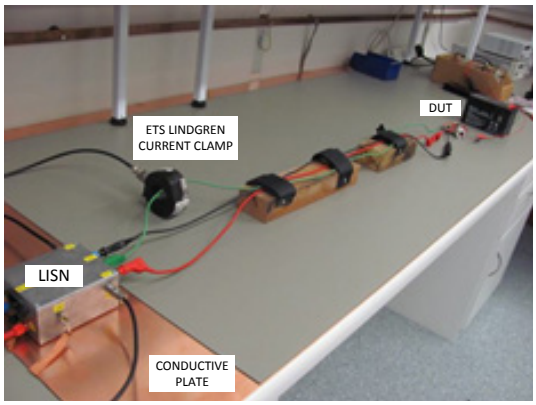

Fig. 15: LISN Bench Setup

The LISN port time signal is recorded and displayed in Fig. 16. This compares to the simulated signal in Fig. 12. Frequencies and amplitudes are slightly off, but the results can be very valuable as a first order high frequency EMC tool

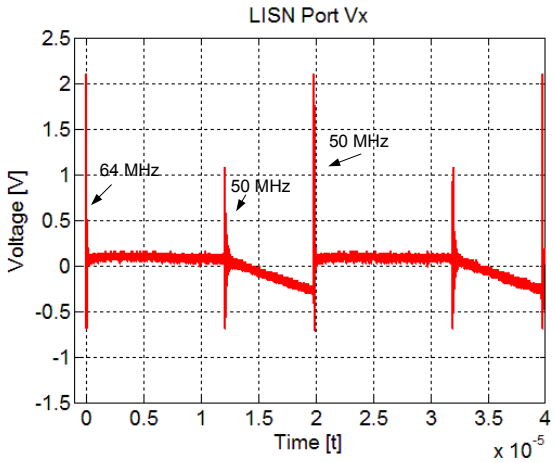

Fig. 16: Noise Voltage Measured at LISN Port

The CM and DM extraction is performed on the time signal in Fig. 16 and an FFT performed. The spectral slopes are displayed in Fig. 17.

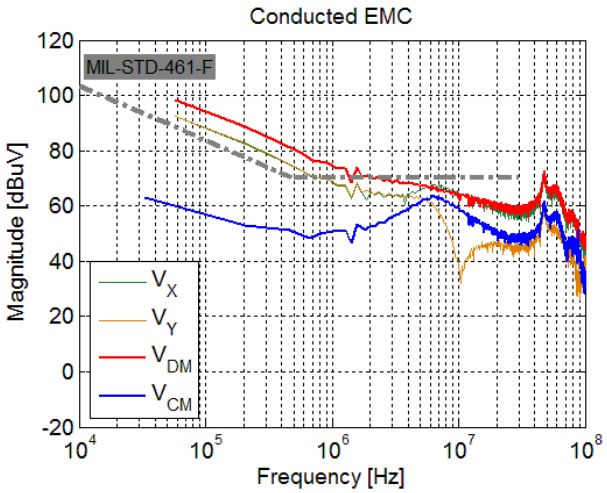

Fig. 17: Prototype FFT Spectrum

Fig. 17 can now be compared to the modelled plot in Fig. 13. The low frequency seems to be very accurate. The high frequency part shows very good comparison to the modelled spectrum. The frequency seems to be accurate although the high frequency amplitudes are about 10 dB off compared to the measurements.

V. CONCLUSION

It was shown and demonstrated that the modern power converters noise levels increase due to the ever increasing switching frequency. It is thus very important to design for EMC.

The traditional analysis method was implemented on the step-down converter, showing that the high frequency effects are poorly represented.

A lumped element model of the step-down converter was created, including the switches and the LISN. Although this technique is presented in literature, accuracy due to the type of CAD packages used did not meet the requirements. PowerSim showed very promising results. It can furthermore be utilized to provide design insight in the power converter.

On both the model and the practical experimentation, common mode and differential mode noise were extracted and compared. This provides further insight into the noise generation and propagation effects. Furthermore, it can aid in optimal filter design.

The lumped element model did not include comprehensive component coupling effects and trace loop effects. As a further insight into the EMC model, these effects can be added for greater accuracy and understanding of the conducted noise effects.

REFERENCES

[1] Jean-Christophe Crebier and Jean-Paul Ferrieux, "PFC Full Bridge Rectifiers EMI Modelling and Analysis—Common Mode Disturbance Reduction," IEEE Transactions on Power Electronics, vol. 19, no. 2, March 2004.

[2] Qian Liu, "Modular Approach for Characterizing and Modelling Conducted EMI Emissions in Power Converters," Ph.D dissertation, Virginia Polytechnic Institute and State University, Blacksburg, Virginia, November 2005

[3] X J. Lai, X. Huang, E. Pepa, S. Chen and T. W. Nehl, "Inverter EMI modelling and simulation methodologies," IEEE Transactions on Industrial Electronics, Vol. 53, No. 3, June 2006

[4] Yan Zhou, Yongfa Zhu, Qingliang Song, Zhaoguo Jin, Dan Yang and Xuequan Yu, "Prediction and reduction of electromagnetic conducted emission in active clamp forward converter", IEEE Electromagnetic Compatibility (EMC), Page(s): 729-733, 2011

[5] K.R.A Britto, RVimala, R. Dhanasekaran, B. Saranya, "Modeling of conducted EMI in flyback switching power converters", IEEE, Electronics and Control Engineering (ICONRAEeCE), Page(s): 377-383, 2011

[6] Xuejun Pei, Kai Zhang, Yong Kang and Jian Chen, "Analytical Estimation of Common Mode Conducted EMI in PWM Inverter", IEEE IAS 2004

[7] Tim Williams, "EMC for Product Designers", Fourth Edition, 2007, Published by Elsevier Ltd

[8] Vimala, R., K.Baskaran and N.Devarajan, "Modeling and Filter Analysis of Differential Mode EMI for Switching Power Converters", European Journal of Scientific Research (EJSR), Vol.52, No.4, pp.553-568, 2011

.